THE JOURNAL OF PHYSICAL CHEMISTRY C
A JOURNAL OF THE AMERICAN CHEMICAL SOCIETY

pubs.acs.org/JPCC
Article

NMR Relaxation Dispersion of Liquids Adsorbed on Modified Surfaces of SBA-15 Mesoporous Silica

Bulat Gizatullin, Carlos Mattea, Siegfried Stapf,* Till Wissel, and Gerd Buntkowsky

Cite This: J. Phys. Chem. C 2024, 128, 8785−8796

Read Online

ACCESS | Metrics & More | Article Recommendations | Supporting Information

ABSTRACT: The NMR relaxation dispersion of ^{1}H and ^{2}H nuclei in water and alkanes was studied in mesoporous SBA-15 silica in its native state and with modified internal surfaces. By comparison with silica gel of comparable characteristic pore size, a qualitative agreement of the relaxation dispersion was found. In the absence of detectable amounts of paramagnetic centers, intramolecular relaxation is approximated by the model of Reorientations Mediated by Translational Displacements (RMTD), which assumes rigid molecules diffusing along curved surfaces and experiencing long-term memory of their relative orientation due to their polarity. For all liquids, significant relaxation dispersion is found so that the vanishing polarity of alkanes does not allow the assumption of a negligible surface interaction. The difference in dispersion shape between ^{1}H and ^{2}H nuclei, relaxing by dipolar and quadrupolar mechanisms, respectively, allows the reconstruction of the intermolecular contribution to relaxation, which has not yet been studied systematically in porous media. A model based on the relative contributions of intra- and intermolecular interactions as well as hydrogen exchange with OH- and NH_2-groups is presented.

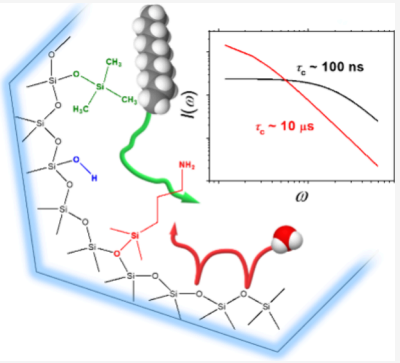

1. INTRODUCTION

A crucial role in the development and implementation of the application of porous materials is a deep understanding of fundamental dynamics processes related to the adsorption, filtration, catalytic activity, etc. silica is one of the most used porous materials.[1−6] The variety of porous structures, pore sizes, and possible surface modifications make silica the best option for the model adsorbent to study fundamental processes at the solid−liquid interface. One of the differences of silica in comparison with, e.g. porous carbon or porous metal oxides is the hydroxyl-enriched, polar surface, which allows modifications by chemical bonding or physical adsorption of different functional groups or complexes, changing the hydrophilic properties, as well as polarity, of the silica surface.[7−13]

The frequency dependence of the NMR relaxation times, or so-called relaxation dispersion, of molecules in contact with solid interfaces has been studied in some detail for at least three decades.[14−22] While relaxation times measured at a particular fixed magnetic field strength, or Larmor frequency, and even different temperatures provide limited information about the dynamics of molecules, probing the full spectral density function over a wider range of frequencies allows for the modeling of the complete spectrum of reorientations of adsorbed molecules, or rather of the attached nuclear spins. Although time scales typical to free molecular rotation, i.e. on the order of picoseconds, cannot be accessed directly, it was found that very slow processes extending to milliseconds become observable in mesoporous media where the surface-to-volume ratio is particularly large, and the surface structure is often characterized by regular or random topologies with particular local curvatures.[23−25] NMR, dielectric spectroscopy, and neutron scattering are among the very few methods that are able, at least in principle, to access these dynamics. Dielectric spectroscopy, however, has only rarely been applied and is limited to molecules with permanent dipoles; neutron scattering is sensitive to rather short time scales, as is the case for MD simulations even up to these days. The interpretation of the NMR relaxation dispersion (NMRD), therefore, must rely on the choice of suitable models and approaches to verify or falsify the latter. One possible approach is the systematic variation of parameters such as surface polarity, molecular polarity, and target nuclei. In this study, all three aspects are varied in order to assess the validity of existing models for molecular interactions with the surface.

One successful approach, also known as Reorientations Mediated by Translational Displacements, or RMTD model, developed by Kimmich et al.,[17,18] since the 1990s assumes the limiting cases of a "clean" surface, entirely lacking paramagnetic impurities, of adsorbed molecules being either polar or nonpolar, representing the case of "strong" or "weak" interaction with a polar surface; and not taking into account

Received: January 30, 2024
Revised: April 22, 2024
Accepted: May 7, 2024
Published: May 15, 2024

https://doi.org/10.1021/acs.jpcc.4c00645
J. Phys. Chem. C 2024, 128, 8785−8796

the particular nature of the interaction, which may be either of Coulomb or van der Waals type or include hydrogen exchange. In this model, molecules were considered as rigid entities without internal dynamics. With these assumptions, it could be shown that the relaxation of polar molecules on the surfaces of porous glasses, pyrogenic silica, ceramics, and certain types of metal-free clays is described by pure molecular reorientation with respect to the surface, which can be expressed as a distribution of surface modes corresponding to a distribution of radii of curvatures. Relaxation dispersion of nonpolar molecules was generally observed to be much weaker but was not considered in the majority of these studies.[26] For very small pores, such as in Vycor porous glass of 4 nm nominal pore diameter, the assumption of vanishing relaxation dispersion for any kind of molecule does not hold any more.[22]

Most studies to date were carried out on randomly structured mesoporous media, even though they possess defined averaged structural dimensions, such as pore diameters or radii of spherical particles, such as in pyrogenic silica. Molecules in micropores, typically 1 nm or less in size, involve partly coherent reorientations of a small number of molecules and require a different type of modeling approach. In this study, we aim to compare NMR relaxation dispersion in intermediate pore sizes, which allow the presence of a bulk-like phase of randomly distributed molecules away from the interface but with a well-defined geometry. This geometry is given by the approximately cylindrical pore shape of SBA-15 silica[27] with well-defined pore diameters in the range of several nanometers. SBA-15 can be considered chemically similar to pyrogenic silica; therefore, a comparison of the adsorption and NMR properties seems justified.

In order to identify the relative importance of polarity and relaxation mechanism, we compare water and linear alkanes, together with their deuterated homologues, as the fluid phase in SBA-15 with a 6.1 nm pore diameter. Furthermore, the native polar surface of SBA-15 was modified to change its interaction and polarity; this modification was included in the preparation process, resulting in sets of SBA-15 samples with minimally larger pore sizes of 6.7 nm. To the best of our knowledge, no systematic NMR relaxometry study has been carried out with this type of silica. The defined modification of its surface, in combination with the well-known structure, provides a novel approach at testing the existing dynamics models to quantify the relative importance of intra- vs intermolecular relaxation contributions, as well as the role of hydrogen exchange that has not been taken into consideration for comparable materials. In particular, the geometrical and interaction effects added by the surface modifications are of interest for gaining further insight into relaxation processes.

2. THEORETICAL BACKGROUND

NMR relaxation is sensitive to the temporal fluctuations of the local interactions at the position of the spin-bearing nuclei; the distribution of these fluctuations is expressed by the spectral density function $I(\omega)$ and those processes are most efficient for relaxation, i.e. for inducing flips of the related nuclear spins, which are of the Larmor frequency ω_n at the given external magnetic field B, $\omega_n = \gamma_n B$ with γ_n being the gyromagnetic ratio of the nucleus. The dominating contribution to these fluctuations is frequently given by dipolar interactions for $I = 1/2$ spins, such as ^{1}H, and by quadrupolar interactions with the gradient of the local electric field for $I > 1/2$ spins, such as ^{2}H. For dipolar and quadrupolar relaxation, the formal relation of relaxation rates R_1 and R_2 are expressed by identical superpositions of spectral density functions:

$$R_1 = T_1^{-1} = C_i[I(\omega_n) + 4I(2\omega_n)] \quad (1)$$

$$R_2 = T_2^{-1} = 0.5C_i[3I(0) + 5I(\omega_n) + 2I(2\omega_n)] \quad (2)$$

with T_1 and T_2 as respective spin−lattice and spin−spin relaxation times, C_i as a prefactor considered as $C_{dip} = (\mu_0/4\pi)^2\gamma^4\,\hbar^2 I(I+1)/(5r^6)$ for homonuclear dipolar relaxation, and $C_{quad} = (3/80)(e^2qQ/\hbar)^2\,(1+\eta^2/3)$ for quadrupolar relaxation, respectively, where I is the spin quantum number, r is the internuclear distance, Q is the quadrupolar moment, q is the electric field gradient, and η is the asymmetry parameter of the electric field. The structural identity of these equations allows one to test whether relaxation is dominated by intramolecular processes such as rigid-body rotation, in which case the frequency dependence of T_1 and T_2 is the same for a molecule containing ^{1}H and/or ^{2}H, and the prefactors can be calculated from known parameters or even derived from scaling arguments of bulk liquids, where the frequency dependence disappears. Further on, taking the ^{2}H relaxation data as a reference, in order to obtain intermolecular relaxation contribution, the measured ^{2}H NMRD can be subtracted from the ^{1}H NMRD using the following equation:

$$T_{1,inter}^{-1} = T_1^{-1}(^1H) - CT_1^{-1}(^2H) \quad (3)$$

where $C = T_{1b,intra}^{2H}/T_{1b,intra}^{1H}$ is a prefactor related to the ratio of the intramolecular relaxation time of ^{1}H and ^{2}H in bulk liquids.[28] While assuming the dominating intramolecular contribution of deuteron relaxation, $T_{1b,intra}^{2H}$ relaxation times of bulk deuterated liquids are measured directly, the $T_{1b,intra}^{1H}$ was calculated taking into account the measured values of T_1 and literature data about the intramolecular relaxation contribution to the ^{1}H relaxation of bulk water ($T_{1b,inter}^{1H}/T_{1b,intra}^{1H} = 3$) and n-decane ($T_{1b,inter}^{1H}/T_{1b,intra}^{1H} = 1.4$).[29] Thus, in the current contribution, the corresponding intermolecular NMRD, which is further fitted using the translational dynamics model with two contributions, has been obtained using subtraction of ^{1}H and ^{2}H NMRDs according to eq 3. It should be noted that for the sake of fitting accuracy the subtraction procedure can be omitted, and the corresponding fitting is carried out simultaneously with a combination of eqs 1 and 3. However, the implementation of the subtraction procedure and presenting the separated intermolecular NMRD were dictated by the intention of showing the reader the difference in shape and position in comparison with intramolecular NMRD as well as among the samples with surface modifications.

As mentioned above, dipolar relaxation consists of an intra- and intermolecular contribution,

$$T_1^{-1} = T_{1,intra}^{-1} + T_{1,inter}^{-1} \quad (4)$$

where each of them represents a weighted sum of interactions of the target spin with all other spins in the same or in neighboring molecules, respectively. Note also that the spectral density of heteronuclear dipolar relaxation has a different structure. This includes nuclear-electron relaxation as a special case.[27,30]

The spectral density function $I(\omega)$ in eqs 1 and 2 is the Fourier transform of the autocorrelation function of magnetic field fluctuations as are brought about by molecular orientations, and is straightforwardly expressed for simple

https://doi.org/10.1021/acs.jpcc.4c00645
J. Phys. Chem. C 2024, 128, 8785−8796

situations such as rigid rotation or two-site exchange as Lorentzian spectral density function:[27]

$$I(\omega) = \frac{\tau}{1 + \omega_n^2\tau^2} \tag{5}$$

where ω_n is Larmor frequency and τ is the correlation time of dynamics process, such as rotation, exchange, etc. In other cases, it has been computed based on the known parametrization of molecular motion. For the case of molecules in the presence of solid surfaces, as discussed in this work, two main approaches have been developed that predict and explain NMR relaxation.

While eq 5 assumes a single correlation time, the presence of a distribution of correlation times is more realistic in the presence of a generally heterogeneous surface. A mathematically convenient way to introduce a distribution of correlation times is using the Cole-Davidson spectral density form:[31,32]

$$I_{CD}(\omega, \tau_{CD}) = \omega_n^{-1}\frac{\sin[\beta \arctan(\omega_n\tau_{CD})]}{[1 + \omega_n^2\tau_{CD}^2]^{\beta/2}} \tag{6}$$

where $0 < \beta \leq 1$ (for $\beta = 1$, the equation to becomes Lorentzian function, see eq 5). The Cole-Davidson function is a well-known form of spectral density for describing intramolecular dynamics in high-viscosity liquids. In the current contribution, eq 6 is used to describe the dynamics related to exchange between two sites with a distribution of exchange times and respective relaxation contribution, which is described with eq 1 with the corresponding prefactor C_{CD}, similarly to C_{dip} and C_{quad}, and characteristic time τ_{ex} (see Table 2).

In the presence of a significant concentration of paramagnetic centers, such as radicals or metal ions in close vicinity of a surface, dipolar relaxation will be entirely dominated by molecular encounters with these centers and the resulting interaction between nuclear spins and the spins of unpaired electrons with their much larger magnetic moment.[13] $I(\omega)$ is then given by the probability of molecules hitting one of these centers as they diffuse close to the surface, effectively reducing 3D Brownian motion to a 2D surface diffusion being reflected in $I(\omega)$.[19,33,34] This model has been successfully applied in natural rocks or cements that can contain large amounts of paramagnetic ions such as iron or manganese.

Artificial porous media, such as silica gel, porous glass, and even a number of zeolites and metal−organic frameworks, contain only minute amounts of paramagnetic centers, so that the aforementioned process is inefficient. Relaxation then occurs by the effect of geometrical restrictions, i.e., by the degree that the presence of the solid interface affects the free rotational and translational dynamics of the liquid molecule. Furthermore, direct interactions such as Coulomb or van der Waals forces, hydrogen exchange, or even valence bonding can affect relaxation additionally, the latter also resulting in a deviation of the macroscopic diffusion properties. However, in most cases, liquid molecules on surfaces retain a large degree of mobility while experiencing a change of local orientation, which directly enters into the autocorrelation function and, therefore, also $I(\omega)$. The mechanism dominating the relaxation of adsorbed liquids in porous media with a negligible amount of paramagnetic species on the surface of the porous material is called Reorientations Mediated by Translational Displacements, or RMTD.[16,17] The RMTD model, as discussed earlier in the literature,[16,23] outlines the distinction between two extreme limiting cases of strong and weak interactions of molecules with the surface. Specifically, for polar molecules, the model accounts for the preferential orientation and significant adsorption interaction, primarily attributed to the presence of a high density of surface hydroxyl groups with additional hydrogen bonding effects. Mainly, polar molecules, such as water and acetone, often meet the requirements for strong adsorption and relaxation ruled by RMTD, which has first been shown for water and D_2O.[16] The agreement of both ^{1}H and ^{2}H nuclei NMRDs in these molecules can be seen as proof of the dominating intramolecular nature of the relaxation process, at least in the systems similar to the porous glass of 30 nm pore size, which was the object under study.[16] On the other hand, nonpolar molecules, such as alkanes, tend to adhere to the weak interaction limiting case, exhibiting minimal surface adsorption and resembling a mirror surface with negligible relaxation mechanisms.[14,16,35] Alternatively, when considering an inorganic surface coated with a hydrocarbon layer, the presence of alkanes exhibited a comparable NMRD once the Al_2O_3 surface was partially modified by the organic substance. However, a consistent flat NMRD was observed with the untreated surface.[36] Furthermore, the research findings indicated that the ^{1}H NMRD of water remained notably pronounced, irrespective of the coke content. Notably, the surface fractal dimension, as determined by the RMTD model, exhibited a consistent change following the surface roughness, as determined by independent methods. Recent investigations have also corroborated these findings in both native and oil-treated rocks.[28,37]

In order to enable a quantitative prediction of the spectral density function based on the RMTD model, it becomes necessary to parametrize the surface roughness. This procedure might involve making assumptions about a singular radius of curvature or considering a fractal distribution of surface modes k, denoted by a function $S(k) = bk^{-\chi}$,[18] where $0 < \chi < 1$. The condition $\chi = 0$ represents the equipartition of surface modes. If normal diffusion is considered along the surface, the Gaussian form well describes the probability density of molecular displacements, characterizing reorientations by the Fourier-transform equivalent of the surface curvature in terms of wavenumbers k and respective characteristic time $\tau_k = (Dk^2)^{-1}$. Assuming that all modes k are equally weighted between k_{min} and k_{max}, the relaxation via RMTD is expressed as[17,38,39]

$$R_{1RMTD} = C_{RMTD}\left\{\frac{1}{\omega_n^{1/2}}\left[f\left(\frac{\omega_{\max}}{\omega_n}\right) - f\left(\frac{\omega_{\min}}{\omega_n}\right)\right] + \frac{4}{(2\omega_n)^{1/2}}\left[f\left(\frac{\omega_{\max}}{2\omega_n}\right) - f\left(\frac{\omega_{\min}}{2\omega_n}\right)\right]\right\} \tag{7}$$

with

$$f(x) = \arctan(\sqrt{2x} + 1) + \arctan(\sqrt{2x} - 1) - \operatorname{arctanh}\left(\frac{\sqrt{2x}}{x + 1}\right)$$

and $\omega_{min,max} = 2\pi/\tau_{k_{max,min}}$, where $\tau_{k_{max}}$ and $\tau_{k_{min}}$ are characteristic times corresponding to k_{min} and k_{max}. The prefactor C_{RMTD} is related to the residual dipole−dipole nuclear interactions in the case of ^{1}H nuclei and quadrupolar interactions for ^{2}H nuclei,

https://doi.org/10.1021/acs.jpcc.4c00645
J. Phys. Chem. C 2024, 128, 8785−8796

which are averaged by local molecular reorientations as well as diffusion processes.

The dynamics processes mentioned above are related to the intramolecular relaxation contributions, while, in general, in order to describe intermolecular contribution to the relaxation dispersion, the translational diffusion must be considered. The force-free-hard-sphere (FFHS) model is commonly used to describe the translational diffusion.[40,41] Further on, corresponding contributions to the relaxation rate are described by eqs 1 and (2) with the spectral density function defined as[40−42]

$$I_{tr}(\omega, z) = \frac{1 + 5z/8 + z^2/8}{1 + z + z^2/2 + z^3/6 + 4z^4/81 + z^5/81 + z^6/648} \quad (8)$$

where $z = \sqrt{\omega_n \tau_{FFHS}/2}$ and τ_{FFHS} is a correlation time defined as

$$\tau_{FFHS} = \frac{d^2}{D_1 + D_2} \quad (9)$$

where d is the minimal distance of approach of interacting spins.[41,43] The d value can be calculated using the van der Waals radii of interacting molecules or functional groups containing interacting spins.[44,45] Further on, D_1 and D_2 as self-diffusion coefficients of the molecules carrying interacting spins, if they belong to the different species, assuming heteronuclear or electron−nuclear interactions.[27,41,46] When the spectral density is defined as in eq 8, the prefactor C_{FFHS} instead of C_{dip} in eq 1 related to the FFHS model is proportional to the spin-density of interacting spins from different molecules and inversely proportional to the minimal distance of approach d (see eq 9).

However, when homonuclear spin−spin intermolecular interactions in similar molecules are considered, the right-hand side of eq 9 turns into $d^2/2D$ with one single diffusional constant. It should be noted that there is no well-established dynamics model describing the above-mentioned process in porous media. One of the problems is that similar molecules are supposed to exhibit restricted translational dynamics in the close vicinity of the solid surface or the proton spins are physically immobilized in surface hydroxyl or other functional groups, while molecules in bulk are still mobile. Thus, one should analyze the translational dynamics considering different diffusion constants or even the distribution of the latter. Moreover, the prefactor in eq 1 related to the translational dynamics model must be corrected, taking into account the relative weight of corresponding fractions and the presence of a solid surface.

Thus, analysis of the NMRD of adsorbed liquids, in general, considers a superposition of several contributions to the relaxation rate:

$$T_1^{-1} = T_{1,RMTD}^{-1} + T_{1,FFHS}^{-1} + T_{1,CD}^{-1} + T_{1,0}^{-1} \quad (10)$$

where $T_{1,CD}^{-1}$ is the relaxation rate related to intramolecular contribution due to the exchange between two sites described by the Cole-Davidson spectral density function (see eq 6) and $T_{1,0}^{-1} = R_{10}$ is the contribution of the fast local dynamics.

3. SAMPLES AND EXPERIMENTS

Preparation of SBA-15 and Fumed Silica Samples. The substances were used without any further purification unless explicitly mentioned. Tetraethyl ortho silicate (98%, TEOS) and Triethoxymethylsilane (98%, TEMS) were purchased from Acros. Pluronic P123 ($M_n \sim 5800$) was purchased from Sigma-Aldrich. Hydrochloric acid (37 wt %, HCl) and ethanol (≥99.8%, EtOH) were purchased from Carl Roth. (3-Aminopropyl)triethoxysilane (98%, APTES) was purchased from ABCR. The fumed silica powder was purchased via Sigma-Aldrich (CAS 112945−52−5). Bidistilled water was used as one of the adsorbates, as well as 99.9% isotopically pure D_2O purchased from Deutero GmbH, Germany. *N*-Decane was purchased from Sigma-Aldrich, and nonane-d20 was obtained from Akademie der Wissenschaften der DDR, Zentralinstitut für Isotopen and Strahlenforschung. All liquids were used without further purification.

The synthesis is based on an optimized protocol of Wang et al.[47] and Zeidan et al.[48] Details of the synthesis procedure for native SBA, SBA-CH_3, and SBA-NH_2 are given in the Supporting Information (SI). The properties of the SBA-15 samples are presented in Table 1. For the details, see the SI.

Table 1. Calculated linker loading from Thermal Analyses and Specific Surface Area and Pore Properties from Gas Adsorption Analysis[a]

Sample	Specific surface area [$m^2\ g^{-1}$]	Pore volume [$cm^3\ g^{-1}$]	Average pore diameter [nm]	Linker loading [$mmol\ g^{-1}$]	Molecule density [nm^{-2}]
SBA	600	0.81	6.1		
SBA-CH_3	798	0.99	6.7	(2.4[b]/5.4[c])	(1.8[b]/4.1[c])
SBA-NH_2	635	0.78	6.7	1.8[d]	1.7

[a]The average pore diameter was calculated as the average value from the BJH and the NLDFT method. For detailed information, see SI. [b]Calculated by TGA. [c]Calculated by carbon content. [d]Calculated by nitrogen content.

Before adding the liquids to the SBA-15 powder, drying was carried out in the vacuum oven for 12 h at 390 K under less than 10 mbar in order to remove residual moisture. In order to prepare SBA-15 samples, the volume of liquids corresponding to 80% of pore volume (see Table 1) was added to each SBA-15 sample in order to avoid bulk liquid between SBA-15 crystallites. The samples were sealed in 10 mm glass tubes and stored for 48 h for even redistribution of adsorbates. The preparation of fumed silica samples was carried out similarly to that of SBA-15 samples. The studied liquids were added to SA380 powder at 2 mL/g for all liquids (H_2O, D_2O, *n*-decane, nonane-d20), which allows obtaining the samples with a homogeneous distribution of liquids without additional manipulations, such as compression or mixing.

Experimental Methods. *FFC NMR.* NMRD experiments were carried out by using an FFC relaxometer (Spinmaster FFC2000, Stelar, Mede, Italy) at magnetic field strengths between 0.1 mT and 0.6 T. For the detection of the NMR signal, the probes were tuned to 16.7 or 3.4 MHz for ^1H and ^2H target nuclei, respectively. The detection field was set at corresponding strengths of 392 and 525 mT for ^1H and ^2H nuclei, respectively. The acquisition was performed with a CPMG pulse sequence with 50 μs echo-time. All measurements were carried out at 293 K.

Solid-State NMR. On a Bruker AVANCE II+ 400 spectrometer, the ^{29}Si and the ^{13}C CP-MAS solid-state spectra

https://doi.org/10.1021/acs.jpcc.4c00645
J. Phys. Chem. C 2024, 128, 8785−8796

were measured at room temperature. A 4 mm double resonance probe was used, corresponding to a frequency of 400.13 MHz for ^{1}H, 79.49 MHz for ^{29}Si and 100.61 MHz for ^{13}C. A recycle delay of 2 s with a contact period of 1.5 ms was employed. For decoupling the protons, tppm-15 decoupling sequence[49] was applied during the analyses With respect to tetramethylsilane (0 ppm), kaolin (−92.5 ppm) and adamantane (−38.5 ppm) were utilized as external standards for ^{29}Si and ^{13}C, respectively.

Elemental Analysis (EA). The EA analyses were conducted on a VarioEL III CHN instrument from Elementar. In a typical measurement, 1−3 mg of the sample is combusted in a tin capsule under an oxygen atmosphere. During the analysis the resulting gases CO_2, H_2O and NO_x, which gets reduced by elemental copper, were separated by gas chromatography and were quantified with a thermal conductivity detector (TCD). The calibration was performed with acetanilide, and helium was employed as the carrier gas.

Thermogravimetric Analysis (TGA). A TG 209 F3 Tarsus from NETZSCH was employed for the thermogravimetric analyses. In an aluminum oxide crucible, approximately 5 mg of the sample is weighted. Before the decomposition of the organic proportion, a predrying step is performed. The temperature is raised from 40 to 100 °C and held for 75 min. Subsequently, the temperature is raised again to 700 °C with a heating rate of 20 K/min. To ensure complete degradation of the organic content, the temperature is held at 700 °C for 30 min.

Gas Adsorption Analysis. The porosity and specific surface area were characterized by performing gas adsorption analysis at 77 K on a Thermo Fisher Scientific Surfer Brunauer−Emmett−Teller (BET) analyzer with nitrogen as the adsorbent. The specific surface area was obtained by analyzing the curve in the range p/p^0= 0.03−0.35 with the BET method. To receive the pore size distribution two methods, Barrett−Joyner−Halenda (BJH) and NLDFT, were employed and the mean of both results was calculated.[50] With the BJH method, the desorption branch of the isotherm in the p/p^0 range between 0.1 and 0.95 was examined, while for the calculation with the NLDFT method, a cylindrical silica at 77 K was assumed. The determination of the pore volume was done by the Gurvich method at the value of p/p^0 = 0.95.

4. RESULTS AND DISCUSSION

In order to provide an overview of the trends in relaxation as a consequence of surface modification, all experimental results on SBA are presented in Figures 1a−c for native SBA-15, SBA-CH_3 and SBA-NH_2 silica, respectively. The dispersion for water follows a sigmoidal shape which has been found before for similar materials, such as silica surfaces,[18,21,23] and is somewhat different from the power-law behavior more typical for porous glasses.[14,16,35] This shape will be discussed in terms of the RMTD processes below.

As a first criterion, the total range of dispersion−i.e. the ratio between relaxation times at the highest and lowest Larmor frequency, is larger for water than for alkanes besides in the SBA-CH_3 samples. This ratio, however, remains somewhat arbitrary since a plateau of T_1 is not reached at high frequencies, indicating that fast processes above some 10^7 Hz remain relevant for relaxation; on the other hand, data approach a plateau at low frequencies. T_1 relaxation times for ^{2}H nuclei are always shorter than those of ^{1}H for the equivalent molecules, in agreement with the same observation

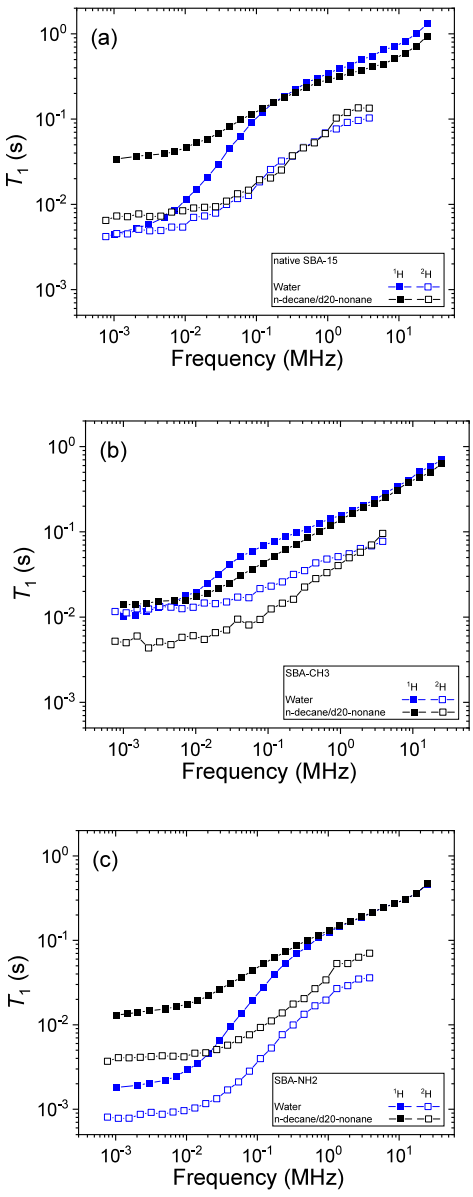

Figure 1. ^{1}H (solid) and ^{2}H (open symbols) NMRD of water (blue), *n*-decane (black) and D_2O and d20-nonane in SBA-15 native (a), SBA-CH_3 (b), and SBA-NH_2 (c).

in bulk liquids. Tentatively normalizing these values by the frequency-independent bulk relaxation times T_1/T_{1bulk}, which eliminates the different prefactors in eqs 1 and 2, leads to almost identical values above 10 MHz but to different trends toward lower frequencies: the *normalized* relaxation times T_1/T_{1bulk} become longer for ^{2}H in water, but shorter or similar for ^{2}H in alkanes (see Figure S1 in the SI). Note that this normalization is an approximation and only makes sense if intramolecular relaxation contributions dominate, since the additional intermolecular contribution possible for ^{1}H nuclei is expected to have a different frequency dependence compared to that of the intramolecular part. Nevertheless, this observation already provides a hint to the presence of intermolecular interactions; this has not been found, for instance, for water in porous glass.[16]

Note that surface modification has a minor effect on the NMRD of alkanes—with the exception of the native SBA-15, which features T_1 times of ^{1}H in *n*-decane more than twice

https://doi.org/10.1021/acs.jpcc.4c00645
J. Phys. Chem. C 2024, 128, 8785−8796

longer than in the modified samples—whereas the variation for water is very pronounced for both ^{1}H and ^{2}H, suggesting that both modifiers, CH_3 groups and APTES spacers with their NH_2 groups attached, affect the interaction of water with the surface. On a qualitative level, these trends can be interpreted: surface modification reduces OH-group density and, therefore, the opportunity of water molecules to interact with the surface, become preferentially oriented, and possibly form hydrogen bonds and/or exchange hydrogen atoms. Replacing hydroxyl groups with methyl groups reduces surface relaxivity, particularly at low frequencies, T_1 becomes longer; APTES, on the other hand, in SBA-NH_2 sample, introduces amino groups as further polar groups, and this effect, combined with a possible steric hindrance due to the presence of linkers, leads to shorter T_1. For the nonpolar alkanes, the presence of polar groups is not relevant by the same amount, and the small differences may be attributed to steric hindrance or a different type of interaction with the added methyl and methylene groups.

Figure 1a shows *native* SBA-15 with a pore diameter of 6.1 nm (see Table 1). The surface contains OH-groups, which results in a strong interaction with water and, as a working hypothesis, a much weaker interaction with alkanes. In fact, the limit of weak interaction in the RMTD model suggests the absence of any T_1 dispersion due to the surface-induced molecular orientation. This is certainly an approximation that is never fully observed since the presence of interfaces always provides mechanisms for slowing down molecular mobility and, therefore, leads to shorter relaxation times. However, the observation that ^{2}H relaxation of D_2O and nonane-d20 is almost identical comes as a surprise; in fact, this is the first time such a behavior is reported. For ^{1}H nuclei, a difference in the dispersion is found but it becomes apparent only below a Larmor frequency of about 0.1 MHz. Whereas dispersion is similar for the two alkanes, though somewhat steeper in the intermediate frequency range 0.1−10 MHz, the additional "step" for water is obvious when normalized to the bulk value. This behavior supports the concept of separating the total relaxation rate of ^{1}H nuclei into an intra- and an intermolecular contribution (eq 3) by subtracting ^{2}H relaxation rates, normalized by a prefactor according to eq 1, see below for a detailed discussion.

Two more preliminary conclusions can be drawn from the comparison of these four data sets. First, relaxation at the highest field approaches bulk values (see Figure S1 in the SI), reaching 50% and 80%, respectively, for water and *n*-decane; this suggests that the possible influence of the surface on fast dynamics, predominantly molecular rotation, is relatively small; i.e., the molecule remains freely mobile close to the surface. From the lack of a plateau, it can be expected that at even higher frequencies T_1 must come even closer to its bulk value. This also puts an upper limit to the possible influence of paramagnetic relaxation due to the possible influence of impurities ion the surface. While EPR measurements have not found any indication of unpaired electrons in these samples, Steiner et al.[51] report the presence of such impurities along with shorter T_1 values of water. Both the long T_1 values and the lack of EPR signal indicate the absence of significant amounts (less than 20 pM according to the EPR spectrometer specification) of paramagnetic centers in the samples of this study. Second, water is a hydrogen bond former and is a protic liquid, while alkanes are neither. From the similarity of the shape of the ^{2}H dispersion of D_2O and nonane-d20, even though it might be coincidental, one might conclude that neither hydrogen bonds nor hydrogen exchange plays a major role in the relaxation properties of ^{2}H in native SBA-15, although this may be entirely different for ^{1}H nuclei.

Figure 1b presents the results for the modified SBA-CH_3 silica. In a simplistic scenario, CH_3-groups replace OH-groups and render the surface nonpolar while at the same time suppress hydrogen exchange. This should lead to a less pronounced dispersion for water. It is estimated (Table 1) that the surface density of CH_3-groups is between 2.4 and 5.4 per nm^2, which would be equivalent to the majority of OH-groups being replaced. Indeed, the low-field relaxation times of ^{1}H nuclei increase about 2-fold for water (see also Figure 1), but the shape of the dispersion changes drastically and becomes much flatter. ^{2}H NMRD of D_2O follows a similar trend. For alkanes, on the other hand, T_1 points in the opposite direction and becomes shorter by a similar amount for ^{1}H, and to a smaller degree also for ^{2}H. This suggests a stronger, but so far unspecified, interaction of the nonpolar adsorbate with the nonpolar surface, similar to what has been observed earlier in catalytic particles covered with hydrocarbon residue.[36]

It should be noted that ^{2}H relaxation times are becoming longer than those of ^{1}H in water at low fields; normalizing T_1 to its bulk value again, this is reflected in an up to 8 times longer relaxation time for ^{2}H at low frequencies, whereas the normalized relaxation times in alkanes are very similar between ^{1}H and ^{2}H across the whole frequency range. All of this suggests a significant intermolecular relaxation contribution for the ^{1}H nuclei in water. Neglecting any possible impurities in the samples, this leaves the CH_3 protons as the most likely culprit for the additional relaxation process of water protons.

Figure 1c shows the NMRD data for the SBA-NH_2 sample, modified with APTES. These samples have a slightly larger pore size (6.7 nm compared to 6.1 nm), which might alter the shape of the dispersion by a small amount. Some OH-groups were replaced by APTES spacers that are terminated by NH_2-groups, with the latter also being polar and allowing hydrogen exchange. The exact ratio of the OH- and NH_2-groups is not known, however. The APTES spacers themselves contain protons and may potentially act as relaxation partners; at the same time, they constitute a certain degree of steric hindrance. It has been shown[52] that, bound to the surface, APTES tend to extend into the liquid phase when water is the adsorbed component, but their behavior in alkanes has not been studied yet. The calculated density is about 1.7 linker units per nm^2 which is rather high; assuming typical OH-groups densities for silica materials, this would suggest that between 25% and 50% of OH-groups are replaced by NH_2-groups. Furthermore, the NH_2-groups probably possess a higher mobility than the surface-bonded OH groups, while on the other hand, the presence of the ^{14}N quadrupolar nucleus drastically shortens the relaxation time of the bonded hydrogen atoms, so that a simple comparison of the interactions of adsorbate molecules with polar surface groups is not possible without further knowledge about their respective NMR properties.

The T_1 dispersions of the SBA-NH_2 samples are indeed almost identical to those of the native SBA, but all curves appear to be shifted vertically as can also be seen in Figure 1. APTES modification leads to between 2.5- and 3.5-times shorter relaxation times for ^{1}H nuclei, slightly more for water when compared to *n*-decane. For ^{2}H data, the trend is similar but amounts to a factor of less than 2 for the alkane and up to 5 for D_2O, with a change of the curvature for the latter

https://doi.org/10.1021/acs.jpcc.4c00645
J. Phys. Chem. C 2024, 128, 8785−8796

becoming obvious. If the NMRD is shifted parallel in a double logarithmic scale, the reason can be in the changing of prefactor in eq 1, suggesting that molecular reorientation or translational diffusion takes place on similar time scales in both sample types. In the case of intermolecular relaxation due to translational diffusion, the prefactor changes can be assigned to the variation in spin density due to the surface proximity or protons of the functional groups.

Pyrogenic silica is a well-studied material that is easily available and has been described in the literature in the context of NMR relaxation. Due to its assumed chemical similarity to SBA-15, we have performed additional experiments in order to verify whether comparable trends can be observed when bringing water and alkanes into contact with silica. By coincidence, the nominal particle diameter of 7 nm is very similar to the pore diameter of SBA-15; however, contrary to earlier publications, the silica samples were not intensively compressed so that the water content was about 30% by volume; i.e., the surface to volume ratio is larger than for SBA-15 so that, assuming fast exchange between surface and bulk-like liquid, the resulting relaxation times are longer.

Figure 2 compares relaxation dispersion data for SBA-15 and SA380 silica in the untreated state. Water NMRD data are

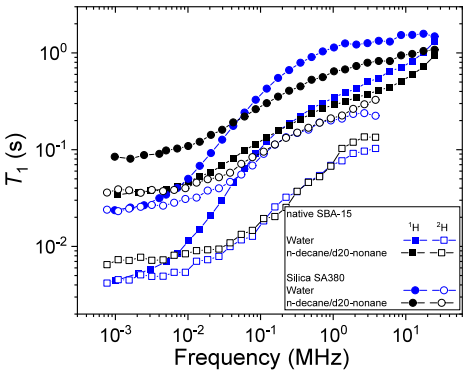

Figure 2. Comparison of ^{1}H (solid) and ^{2}H (open symbols) NMRD of corresponding liquids adsorbed on SBA-15 and fumed silica surfaces.

indeed similar; i.e., the ^{1}H relaxation becomes shorter below 0.1−1 MHz when compared to ^{2}H, so there are possibly relevant intermolecular relaxation processes in this frequency range. The flattening toward high frequencies can be attributed to the crossover toward bulk dynamics because of the lower surface-to-volume ratio.

The normalized alkane data (see Figures S1−S3 in the Supporting Information), however, are almost identical between ^{1}H and ^{2}H, suggesting negligible intermolecular contributions. In any case, this is a smaller effect that was observed for SBA-15. A possible explanation may be in the different pore shapes of the two substances, leading to different geometric hindrance.

Model Comparison for ^{1}H and ^{2}H Relaxation. In order to provide a comparison with the existing models, the following assumptions have been made:

(i) Relaxation is purely intramolecular for ^{2}H nuclei (quadrupolar relaxation), and consists of a sum of intra- and intermolecular contributions for ^{1}H nuclei (dipolar relaxation)

(ii) Dynamical processes causing the intramolecular relaxation are identical for ^{1}H and ^{2}H in comparable molecules

(iii) Chemical exchange affects both nuclei in the same way for water, and no exchange exists in alkanes

(iv) Reorientations Mediated by Translational Displacements (RMTD) is considered as a valid model for water relaxation; tentatively, it is also supposed for alkanes; the model assumes a preferential orientation of the molecules with the surface.

In these assumptions, the isotope effect is neglected, i.e., the somewhat slower dynamics of ^{2}H compared to ^{1}H as well as the different molecular weights; the choice of *n*-decane and *n*-nonane-d20 actually has been made to achieve similar molecular weights, and the similarity, within several percent, of the ^{2}H relaxation dispersion has been verified on a sample containing *n*-decane-d22 (data not shown). The formation of hydrogen bonds has not been explicitly taken into account in the models (see discussion), and the separation of the total relaxation rate into two contributions is considered in a general way; i.e., the "intermolecular" contribution may reflect dipolar relaxation with protons of other molecules, protons on the surface, or possibly unpaired electrons, although the latter are ruled out based on the observed results and the lack of a detectable EPR signal in all samples.

In the RMTD model, the simplest assumption of an equipartition of surface modes has been made, since there is no

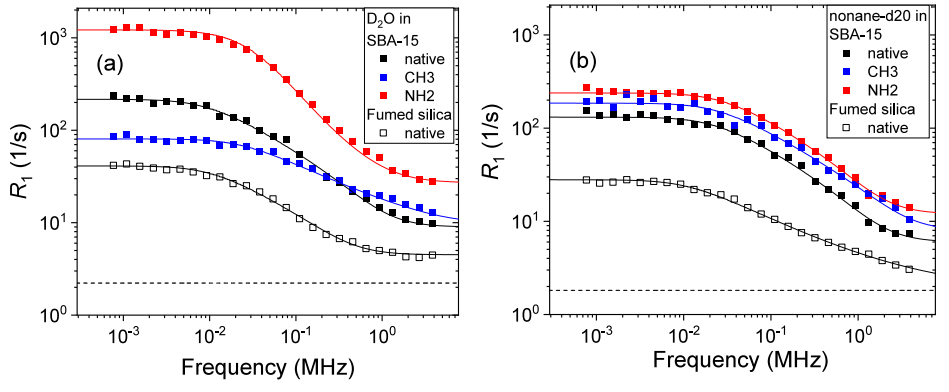

Figure 3. NMRD of the intramolecular contribution to relaxation of water (a) and nonane-d20 (b) adsorbed on SBA-15 and fumed silica presented by ^{2}H NMRD of the respective samples. The lines are fitted using the RMTD model by eq 7 with the addition of the constant contribution $R_{10,intra}$, according to eq 10. The dashed lines correspond to the relaxation rate of bulk liquids.

https://doi.org/10.1021/acs.jpcc.4c00645
J. Phys. Chem. C 2024, 128, 8785−8796

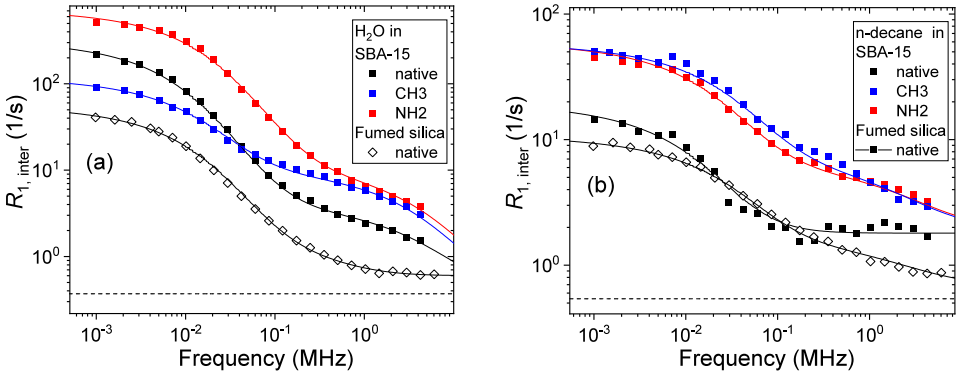

Figure 4. NMRD of intermolecular contribution to ^{1}H relaxation of water (a) and *n*-decane (b) calculated using eq 3. The lines are fitted using NMRD contributions defined by eq 1 with corresponding spectral density related to eq 8. The separated contributions to the total relaxation rate are presented in the Supporting Information. The dashed lines correspond to the relaxation rates of bulk liquids.

Table 2. Fitting Parameters of ^{2}H NMRD of D_2O and Nonane-d20 in SBA Samples as Well as Fumed Silica Using RMTD Model (see eq 7) and Cole-Davidson Spectral Density with eq 6

Silica	Liquid	$R_{10,\ intra}$, s^{-1}	$C_{RMTD} \times 10^3$, s^{-2}	$\tau_{k,max}$, μs	$\tau_{k,min}$, μs	$C_{CD} \times 10^6$, s^{-2}	τ_{ex}, μs
SBA-15, native	D_2O	9	4.7	11.9	0.111	-	
SBA-CH_3		10	2.5	4.5	0.013	-	
SBA-NH_2[a]		26.5	36	7.6	0.263		
		26	2.5[b]	4.5[b]	0.013[b]	1.35	0.48[c]
SBA-15, native	nonane-d20	6	4.5	4.9	0.064	-	
SBA-CH_3		8	6.5	4.5	0.032	-	
SBA-NH_2		12	9.2	4.0	0.068	-	
Fumed silica	D_2O	4.5	0.95	10.3	0.239	-	
	nonane-d20	2.2	0.6	9.5	0.003		

[a]The fitting parameters are shown for the model with only RMTD used for SBA-NH_2 modified samples. [b]Parameters are taken from ones from SBA-CH_3 and fixed for fitting C_{CD} and τ_{ex} parameters. [c]Correlation time $\tau_{ex} = \tau_{CD}\beta$ with $\beta = 0.5$ (see eq 6).

rationale for a self-similar surface structure that would lead to a fractal surface dimension. According to,[18,35] a power-law distribution of surface modes results in a power-law dependence of the relaxation time on Larmor frequency, introducing one more fitting parameter; equipartition therefore constitutes the approach with the smallest number of fitting parameters, such as C_{RMTD}, $\tau_{k,max}$, $\tau_{k,min}$ (see eq 7 and Table 2).

Based on these assumptions, first the RMTD model with equipartition of modes has been fitted to all ^{2}H experimental data (see Figure 3). The corresponding fitting parameters are discussed below. In a second step, a suitably scaled relaxation rate of ^{2}H was subtracted from the total observed relaxation rate of the equivalent ^{1}H nuclei (see the eq 3), where the scaling was tentatively obtained from knowledge of the prefactors of the expressions for the relaxation rates (eqs 1 and 2) and the values of the bulk liquid (see the description below eq 3). The fitting using the FFHS model with several contributions presented in Figure 4 shows good agreement with experimental data despite a possible presence of more complicated processes, which were not taken into account in the current contribution.

As has been outlined in the Theoretical Background Section, the deuteron relaxation rate is described by the RMTD model added to a constant plateau value $R_{10,intra}$ (see eq 10). This value is approximated as the high-frequency relaxation rate limit, which does include the effect of reorientations on frequency scales faster than about 3 MHz. The exact nature of these processes is not considered, here. However, it must be assumed that further restrictions to molecular reorientations are relevant since the observed values are up to ten times higher than the relaxation rates measured in the bulk. The result of this procedure is summarized in Table 2 and presented in Figure 3. Additionally, the Cole-Davidson function (see eq 6) is applied as an additional contribution to the relaxation for the SBA-NH_2 sample with D_2O related to the presence of an exchange water with amino groups. As a contribution related to the RMTD model for the remaining relaxation rate in the SBA-NH_2 sample with deuterated water, the corresponding parameters for the SBA-CH_3 sample with D_2O were used as fixed parameters. In Table 2, therefore, two lines are presented corresponding to the fitting of experimental data for SBA-NH_2 with D_2O using only RMTD and RMTD with an exchange. The lines corresponding to the relaxation rate observed in bulk liquids at 25 MHz are presented to estimate the amplitude of relaxation dispersion related to fast dynamics such as fast individual rotations, which is not detectable due to the FFC technique's frequency range.

Surface diffusion and subsequent reorientation occur between two cutoff modes according to the RMTD model; large k corresponds to short distances/high curvatures, short times, and high frequencies, and vice versa. In principle, the observed cutoff times can be translated into actual dimensions if the surface transport properties can be estimated. The longest time scale varies only over a small range, between 4 and 12 μs, corresponding to frequencies between 13 and 40 kHz. According to the RMTD model, the preferential orientation of the water molecule is induced by its polarity. Replacing surface OH-groups with bulky spacers reduces the ability to carry out trajectories on the surface before being removed from it; also, the presence of CH_3 groups in an environment with much-

https://doi.org/10.1021/acs.jpcc.4c00645
J. Phys. Chem. C 2024, 128, 8785−8796

reduced OH-groups density suggests that the water molecule has a shorter "memory" of its surface trajectory and leaves earlier. This is in agreement with a reduction of the long time scale by up to a factor of 3. The shortest time scale is on the order of 100 ns and varies significantly for water; it is particularly short for the CH_3-modified surface.

The first remarkable effect of the modification, especially pronounced for D_2O in the SBA-NH_2 sample, is a changed relaxivity with the corresponding fitting parameter C_{RMTD}. Thus, if only the RMTD model is considered as a relaxation mechanism, C_{RMTD} is increased for the SBA-NH_2 sample 8 times, while the SBA-CH_3 sample exhibits reducing an amplitude slightly less than two fold. The latter case can be explained by decreasing the number of molecules in the "strongly" adsorbed layer influenced by the surface[39] due to the presence of a methyl group. However, with an 8-fold increase of C_{RMTD} constant in the SBA-NH_2 sample, that logic fails. Moreover, considering any other possible intramolecular relaxation mechanisms, the increasing of the prefactor in eqs 1 and 2 assumes unrealistic changing of the distances between interacting spins within water molecules. The effects of possible structuring of APTES due to the formation of hydrogen bonds either with water or silanol groups in the wet or dry state,[47,53] respectively, must also be pronounced in comparison of water and alkanes NMRD. However, no additional remarkable features on the corresponding NMRD were observed. Thus, the difference in the experimental relaxation rate with corresponding fitting parameters of D_2O in the SBA-NH_2 sample can be explained, e.g. by the presence of exchange between the molecules experiencing reorientation on the surface as well as bulk-like molecules with the proton in NH_2 groups. The latter can be explained by the short relaxation times due to the low mobility and presence of ^{14}N spin.[54] The exchange process is defined by the Cole-Davidson function as a spectral density function in eq 1 (also see Figure SI4c in the SI). The fitting was carried out keeping all parameters fixed that are related to the RMTD model (C_{RMTD}, $\tau_{k,max}$, $\tau_{k,min}$) with values obtained for the SBA-CH3 sample (see Table 2). The prefactor C_{CD} and corresponding correlation time of ∼0.5 μs are presented in Table 2.

The tentative assumption of an RMTD process also for alkanes leads to, at first sight, reasonable numbers, while no exchange effect is considered due to the aprotic character of alkanes. The surface modification does not affect these fitting parameters for nonane-d20, as is reflected in the similarity of the T_1 dispersion curves for the deuterated alkane. The prefactor C_{RMTD} values are up to twice higher for modified samples exhibiting increased interaction of alkane with the surface due to the presence of functional groups.

In general, one of the observations which should be noted here is that the general description of the data using the RMTD model remains possible and reliable even with the modified surface where a high concentration of functional groups is supposed to hinder or sometimes eliminate the specific dynamics on the surface. The latter effect, according to theory, must be indicated as changes in the distribution of wave vectors k, which lead to NMRD shape variation. However, we have not observed dramatic changes in the values of $\tau_{k,max}$ and $\tau_{k,min}$, which correspond to k_{min} and k_{max}, for the sample with APTES on the surface. On the contrary, the amplitude was mostly affected by the corresponding modification of the surface. The current results clearly indicate the need for further studies and the development of more detailed models for surface relaxation, possibly including MD simulations of the actual structure and short-time dynamics of APTES and adsorbates alike.

The next conventional step in the analysis of data obtained considering the RMTD model is converting correlation times $\tau_{k,max}$ and $\tau_{k,min}$ into characteristic length λ corresponding to the distribution of modes due to the surface, using $\lambda = 2\pi/k$ and $\tau_k = (Dk^2)^{-1}$,[39] mentioned above in the theoretical section. The diffusion coefficient D related to RMTD model development was considered as obtained for bulk liquid or as an effective diffusion coefficient in the particular porous material,[16,17] which was similar to the respective value of diffusion coefficient in bulk. The corresponding dimensions obtained in those papers were in good agreement with the pore sizes of the studied porous materials. A similar approach was carried out in liquid crystals[55] and porous polymers,[38] showing good agreement with the size of structures and molecular dimensions in studied systems. However, the estimation of characteristic dimensions ranges using correlation times obtained from the current data and the diffusion coefficient of adsorbed liquid in bulk exhibits the range of characteristic lengths of 30−250 nm on average for the values $\tau_{k,max}$ and $\tau_{k,min}$ in Table 2. The upper value of 250 nm is remarkably higher than the value of pore size of ∼6 nm. That significant discrepancy could be addressed by the pore structure of SBA-15, which is characterized as more ordered in comparison with porous materials in the previous studies. On the other hand, the simple estimation of diffusion coefficient value, which is necessary to match correlation times and corresponding characteristic length to the pore size of SBA-15, gives the value of the order of magnitude of about 10^{-13} m^2/s. This value has not been reported in any diffusion studies with PFG NMR in similar systems. Nevertheless, it should be noted that the time scale of those dynamics must be much shorter than any possible time interval in PFG NMR techniques.

In order to distinguish *intra-* and *inter*molecular contribution to the relaxation, the subtraction of ^2H NMRD from ^1H NMRD with corresponding scaling (see eq 3) has been carried out. However, the straightforward subtraction of the normalized ^2H data is problematic since the resulting intermolecular relaxation rate of *n*-decane is partially negative. This issue may speculatively be addressed by multiplying the subtracted relaxation rate by a factor of approximately 0.5, taking into account the decreased spin density in the immediate vicinity of the surface. Thus, the values of prefactor C in eq 3 are obtained as 0.035 and 0.145 for water and *n*-decane, respectively. The results of the corresponding calculations using eq 6 are presented in Figure 4. Note that simple normalization by the bulk value only works for ^2H while it is known that even in bulk, the intra- and intermolecular contributions to the total relaxation rate for dipolar relaxation of ^1H nuclei are on the same order of magnitude so that the intramolecular part needs to be computed first.

For water, the ^1H relaxation contribution considered as "intermolecular" is of sigmoidal shape and is of similar magnitude as the RMTD-induced intramolecular part. An attempt to fit this dispersion with the translational FFHS model according to eq 8 requires the superposition of two separate processes with two quite different characteristic times and prefactors, τ_{1FFHS}, τ_{2FFHS}, C_{1FFHS}, and C_{2FFHS}, respectively. Similarly to the fitting of intramolecular relaxation presented above, the constant contribution $R_{10,\ inter}$ is considered for the dispersion appearing at higher frequencies outside the FFC

https://doi.org/10.1021/acs.jpcc.4c00645
J. Phys. Chem. C 2024, 128, 8785−8796

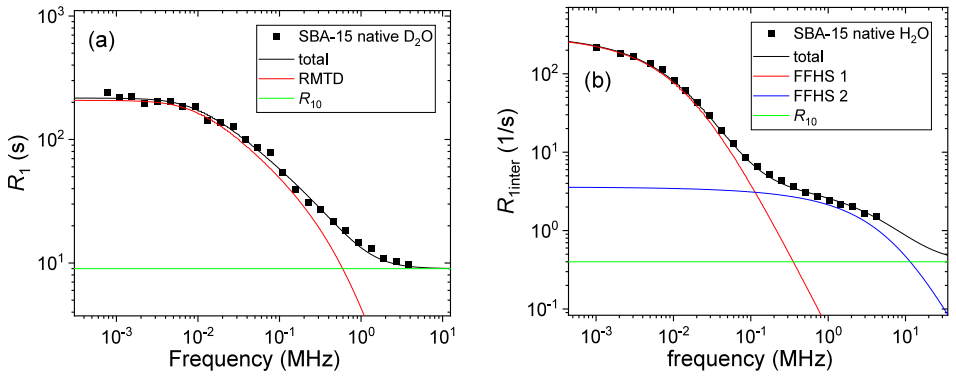

Figure 5. ^{2}H (a) and intermolecular part of ^{1}H (b) NMRD of D_2O and water in native SBA-15. The lines present fitting components related to eqs 1, 7, and 8.

technique range. In Figure 5, the example of fitting both ^{2}H and intermolecular part of ^{1}H dispersions of D_2O and water in native SBA-15 is presented. The fitting component for alkanes as well as modified samples are presented in Figures S4−S7 in the Supporting Information. The results of fitting for the three SBA samples saturated with water and *n*-decane are shown in Table 3 and 4, respectively.

Table 3. Fitting Parameters of the FFHS Model Applied for the Intermolecular Contribution of *Water* NMRD

SBA	C_{1FFHS}, s^{-2}	τ_{1FFHS}, μs	C_{2FFHS}, s^{-2}	τ_{2FFHS}, ns	$R_{10,inter}$, s^{-1}
Pure	2.0×10^6	5.1	12×10^6	10.0	0.4
APTES	9×10^6	2.5	35×10^6	9.2	0.4
CH_3	1.1×10^6	3.2	27×10^6	11.5	0.4
Fumed silica	0.5×10^6	3.5	0.3×10^6	79.6	0.6

Table 4. Fitting Parameters of the FFHS Model Applied for the Intermolecular Contribution of *n-Decane* NMRD

SBA	C_{1FFHS}, s^{-2}	τ_{1FFHS}, μs	C_{2FFHS}, s^{-2}	τ_{2FFHS}, ns	$R_{10,inter}$, s^{-1}
Pure	0.8×10^6	3.2	-	-	1.8
APTES	0.9×10^6	1.9	11×10^6	12.7	2
CH_3	1.3×10^6	1.3	10×10^6	16.0	2
Fumed silica	0.23×10^6	1.3	2×10^6	14.3	0.8

Thus, if we consider FFHS mode, the two separated time scales must be explained. If the correlation time of about 10 ns still can be understood, giving a diffusion coefficient of about 10^{-10} m^2/s while the distance of minimal approach of 3−5 Å is considered (see eq 8), the 1 μs time scale requires additional analysis, since the standard approach to estimate diffusion coefficient exhibits the values of about 10^{-13} m^2/s. The former value of the diffusion coefficient is in good agreement with the literature.[10,50] On the other hand, the value of the diffusion coefficient of 10^{-13} m^2/s corresponds to the order of magnitude of the diffusion coefficient required in RMTD model analysis above to match the pore sizes with dimensions obtained from correlation times. The assignment of those slow processes to any known or new mechanisms or dynamics models is definitely the crucial point of understanding the processes of adsorption and dynamics on the surface, but it is out of the scope of the current study.

Further on, the modifications do not exhibit a remarkable effect on correlation times related to intermolecular relaxation for both water and *n*-decane, while the amplitudes assigned with C_{1FFHS} and C_{2FFHS} constants are changed similarly to those of intramolecular relaxation (see Table 2). However, compared to the latter, an increase in intermolecular relaxation can be explained by the presence of protons of functional groups on the surface, which results in increased spin density in space, where the slowest processes in the system occur. Moreover, considering eq 9, the immobilized species on the surface, i.e., with $D = 0$, will lead to longer correlation times. As for the comparison with intermolecular relaxation in fumed silica, the difference in the amplitude can be explained by the factor related to surface-to-volume ratio.

The modification of the surface of SBA-15 in the case of *n*-decane leads to the similar NMRDs for SBA-CH_3 and SBA-NH_2, differing from native SBA-15 by the factor of 3 with regard to the amplitude of relaxation rate at low frequency and corresponding parameter C_{1FFHS} and C_{2FFHS}.

5. CONCLUSIONS

In the current contribution, the modifications of SBA-15 mesoporous silica are studied by ^{1}H and ^{2}H FFC NMR, etc. The unique combination of a data set for four liquids, water/D_2O and *n*-decane/nonane-d20 are presented in order to reveal the effects of surface modifications on dynamics of different types of adsorbed liquids.

The dynamics changes due to the functionalization of the SBA-15 surface with methyl and amino groups using TEMS and APTES, respectively, are assigned using NMRD and different dynamics models.

The ^{2}H NMRD of both protic and aprotic liquids, presented by D_2O and nonane-d20, is well described using the RMTD model, suggesting the main mechanism of relaxation via preferential reorientations mediated by diffusion in bulk. The functionalization of the surface, on the one hand, leads to reducing the "residential" times of water molecules, probably due to the disruption of surface diffusion via methyl and amino groups. On the other hand, the silica surface with amino groups exhibits signs of accelerating exchange via those groups, which significantly increases the relaxation rate of adsorbed water.

The RMTD model for alkanes, which are aprotic and nonpolar, is tentatively applied for the first time to explain the origin of intramolecular relaxation. The ^{2}H NMRD of nonane-d20, as well as ^{1}H NMRD for *n*-decane, does not exhibit remarkable changes with functionalizing of the SBA-15 surface, explained by the nonpolar and aprotic origin of the former.

https://doi.org/10.1021/acs.jpcc.4c00645
J. Phys. Chem. C 2024, 128, 8785−8796

In order to describe ^{1}H NMRD of water and *n*-decane, two independent contributions are considered, namely, intra- and intermolecular relaxation. The procedure of subtracting ^{1}H and ^{2}H NMRDs from each other with corresponding factors is presented, which results in distinguishing intra- and intermolecular contribution to ^{1}H relaxation. The application of this procedure to the water NMRD exhibits the domination of the intermolecular contribution at low resonance frequencies with up to 90% of the relative weight. On the contrary, the *n*-decane exhibits a relative weight of intermolecular relaxation below 40%. In both liquids in SBA-15, the intermolecular relaxation is described by two contributions with correlation times of approximately 10 μs and 100 ns. The functionalized SBA-15 samples exhibit stronger intermolecular relaxation of *n*-decane due to the increased proton spin density on the surface via addition of methyl and amino groups. The comparison of the NMRD and fitting parameters from the applied model with well-studied fumed silica shows the reliability of the analysis presented in the current contribution.

■ ASSOCIATED CONTENT

Supporting Information

The Supporting Information is available free of charge at https://pubs.acs.org/doi/10.1021/acs.jpcc.4c00645.

Normalized NMRD, results of fitting, additional details of samples preparation, characterization of samples, TGA data and content analysis, gas adsorption analysis and pore size distribution (PDF)

■ AUTHOR INFORMATION

Corresponding Author

Siegfried Stapf − *Dept. Technische Physik II/Polymerphysik, Technische Universität Ilmenau, D-98684 Ilmenau, Germany;* orcid.org/0000-0001-5191-0416; Phone: +49 3677 693671; Email: Siegfried.stapf@tu-ilmenau.de

Authors

Bulat Gizatullin − *Dept. Technische Physik II/Polymerphysik, Technische Universität Ilmenau, D-98684 Ilmenau, Germany;* orcid.org/0000-0002-2385-5621

Carlos Mattea − *Dept. Technische Physik II/Polymerphysik, Technische Universität Ilmenau, D-98684 Ilmenau, Germany;* orcid.org/0000-0002-3051-928X

Till Wissel − *Eduard-Zintl-Institut for Inorganic and Physical Chemistry, Technische Universität Darmstadt, D-64287 Darmstadt, Germany*

Gerd Buntkowsky − *Eduard-Zintl-Institut for Inorganic and Physical Chemistry, Technische Universität Darmstadt, D-64287 Darmstadt, Germany;* orcid.org/0000-0003-1304-9762

Complete contact information is available at: https://pubs.acs.org/10.1021/acs.jpcc.4c00645

Notes

The authors declare no competing financial interest.

■ ACKNOWLEDGMENTS

Financial support by the Deutsche Forschungsgemeinschaft (STA 511/15-1 and -2) and BU 911/24/3 is gratefully acknowledged.

■ REFERENCES

(1) Liu, C. C.; Maciel, G. E. The Fumed Silica Surface: A Study by NMR. *J. Am. Chem. Soc.* **1996**, *118* (21), 5103−5119.

(2) Zaborski, M.; Vidal, A.; Ligner, G.; Balard, H.; Papirer, E.; Burneau, A. Comparative study of the surface hydroxyl groups of fumed and precipitated silicas. I. Grafting and chemical characterization. *Langmuir* **1989**, *5* (2), 447−451.

(3) Morrow, B. A.; McFarlan, A. J. Infrared and gravimetric study of an aerosil and a precipitated silica using chemical and hydrogen/deuterium exchange probes. *Langmuir* **1991**, *7* (8), 1695−1701.

(4) McDonald, R. S. Surface Functionality of Amorphous Silica by Infrared Spectroscopy. *J. Phys. Chem.* **1958**, *62* (10), 1168−1178.

(5) Gallas, J. P.; Lavalley, J. C.; Burneau, A.; Barres, O. Comparative study of the surface hydroxyl groups of fumed and precipitated silicas. 4. Infrared study of dehydroxylation by thermal treatments. *Langmuir* **1991**, *7* (6), 1235−1240.

(6) Li, L.-L.; Sun, H.; Fang, C.-J.; Xu, J.; Jin, J.-Y.; Yan, C.-H. Optical sensors based on functionalized mesoporous silica SBA-15 for the detection of multianalytes (H+ and Cu2+) in water. *J. Mater. Chem.* **2007**, *17* (42), 4492.

(7) Hoffmann, M. M.; Bothe, S.; Brodrecht, M.; Klimavicius, V.; Haro-Mares, N. B.; Gutmann, T.; Buntkowsky, G. Direct and Indirect Dynamic Nuclear Polarization Transfer Observed in Mesoporous Materials Impregnated with Nonionic Surfactant Solutions of Polar Polarizing Agents. *J. Phys. Chem. C* **2020**, *124* (9), 5145−5156.

(8) Liu, J.; Groszewicz, P. B.; Wen, Q.; Thankamony, A. S. L.; Zhang, B.; Kunz, U.; Sauer, G.; Xu, Y.; Gutmann, T.; Buntkowsky, G. Revealing Structure Reactivity Relationships in Heterogenized Dirhodium Catalysts by Solid-State NMR Techniques. *J. Phys. Chem. C* **2017**, *121* (32), 17409−17416.

(9) Steinrucken, E.; Wissel, T.; Brodrecht, M.; Breitzke, H.; Regentin, J.; Buntkowsky, G.; Vogel, M. (2)H NMR study on temperature-dependent water dynamics in amino-acid functionalized silica nanopores. *J. Chem. Phys.* **2021**, *154* (11), No. 114702.

(10) Schrader, A. M.; Monroe, J. I.; Sheil, R.; Dobbs, H. A.; Keller, T. J.; Li, Y.; Jain, S.; Shell, M. S.; Israelachvili, J. N.; Han, S. Surface chemical heterogeneity modulates silica surface hydration. *Proc. Natl. Acad. Sci. U. S. A.* **2018**, *115* (12), 2890−2895.

(11) Di, L.; Hua, Z. Porous Silica Beads Supported TEMPO and Adsorbed NOx (PSB-TEMPO/NOx): An Efficient Heterogeneous Catalytic System for the Oxidation of Alcohols under Mild Conditions. *Advanced Synthesis & Catalysis* **2011**, *353* (8), 1253−1259.

(12) Morrow, B. A.; McFarlan, A. J. Chemical reactions at silica surfaces. *J. Non-Cryst. Solids* **1990**, *120* (1−3), 61−71.

(13) Geppi, M.; Borsacchi, S.; Mollica, G.; Veracini, C. A. Applications of Solid-State NMR to the Study of Organic/Inorganic Multicomponent Materials. *Appl. Spectrosc. Rev.* **2008**, *44* (1), 1−89.

(14) Kimmich, R. Strange kinetics, porous media, and NMR. *Chem. Phys.* **2002**, *284* (1−2), 253−285.

(15) Zavada, T.; Kimmich, R.; Grandjean, J.; Kobelkov, A. Field-cycling NMR relaxometry of water in synthetic saponites: Lévy walks on finite planar surfaces. *J. Chem. Phys.* **1999**, *110* (14), 6977−6981.

(16) Stapf, S.; Kimmich, R.; Seitter, R. Proton and deuteron field-cycling NMR relaxometry of liquids in porous glasses: Evidence for Lévy-walk statistics. *Phys. Rev. Lett.* **1995**, *75* (15), 2855−2858.

(17) Stapf, S.; Kimmich, R.; Niess, J. Microstructure of porous media and field-cycling nuclear magnetic relaxation spectroscopy. *J. Appl. Phys.* **1994**, *75* (1), 529−537.

(18) Kimmich, R.; Weber, H. W. NMR relaxation and the orientational structure factor. *Phys. Rev. B* **1993**, *47* (18), 11788−11794.

(19) Ward-Williams, J.; Korb, J.-P.; Rozing, L.; Sederman, A. J.; Mantle, M. D.; Gladden, L. F. Characterizing Solid−Liquid Interactions in a Mesoporous Catalyst Support Using Variable-Temperature Fast Field Cycling NMR. *J. Phys. Chem. C* **2021**, *125* (16), 8767−8778.

(20) Ward-Williams, J.; Gladden, L. F. Insights into adsorption behaviour of binary liquid mixtures in porous media using fast field cycling NMR. *Magn Reson Imaging* **2019**, *56*, 57−62.
(21) Gizatullin, B.; Mattea, C.; Stapf, S. Radicals on the silica surface: probes for studying dynamics by means of fast field cycling relaxometry and dynamic nuclear polarization. *Magnetic Resonance Letters* **2023**, *3* (3), 256−265.
(22) Stapf, S.; Siebert, N.; Spalek, T.; Hartmann, V.; Gizatullin, B.; Mattea, C. Binary fluids in mesoporous materials: Phase separation studied by NMR relaxation and diffusion. *Magnetic Resonance Letters* **2023**, *3* (2), 108−117.
(23) Kimmich, R.; Stapf, S.; Callaghan, P.; Coy, A. Microstructure of porous media probed by NMR techniques in sub-micrometer length scales. *Magn. Reson. Imaging* **1994**, *12* (2), 339−343.
(24) Anoardo, E.; Bonetto, F.; Kimmich, R. Apparent low-field spin-lattice dispersion in the smectic-A mesophase of thermotropic cyanobiphenyls. *Phys. Rev. E Stat Nonlin Soft Matter Phys.* **2003**, *68* (2 Pt 1), No. 022701.
(25) Mattea, C.; Kimmich, R.; Ardelean, I.; Wonorahardjo, S.; Farrher, G. Molecular exchange dynamics in partially filled microscale and nanoscale pores of silica glasses studied by field-cycling nuclear magnetic resonance relaxometry. *J. Chem. Phys.* **2004**, *121* (21), 10648−56.
(26) Stapf, S.; Kimmich, R.; Seitter, R. O.; Maklakov, A. I.; Skirda, V. D. Proton and deuteron field-cycling NMR relaxometry of liquids confined in porous glasses. *Colloids Surf., A* **1996**, *115*, 107−114.
(27) Kimmich, R. *NMR Tomography Diffusometry Relaxometry*; Springer-Verlag: Berlin, Heidelberg, 1997; p 526.
(28) Gizatullin, B.; Mattea, C.; Shikhov, I.; Arns, C.; Stapf, S. Modeling Molecular Interactions with Wetting and Non-Wetting Rock Surfaces by Combining Electron Paramagnetic Resonance and NMR Relaxometry. *Langmuir* **2022**, *38* (36), 11033−11053.
(29) Singer, P. M.; Asthagiri, D.; Chapman, W. G.; Hirasaki, G. J. Molecular dynamics simulations of NMR relaxation and diffusion of bulk hydrocarbons and water. *J. Magn. Reson.* **2017**, *277*, 15−24.
(30) Solomon, I. Relaxation Processes in a System of Two Spins. *Phys. Rev.* **1955**, *99* (2), 559−565.
(31) Havriliak, S. J. *Dielectric and Mechanical Relaxation in Materials: Analysis, Interpretation, and Application to Polymers*; Hanser Publishers: 1997.
(32) Beckmann, P. A. Spectral densities and nuclear spin relaxation in solids. *Phys. Rep.* **1988**, *171* (3), 85−128.
(33) Benamsili, L.; Korb, J.-P.; Hamon, G.; Louis-Joseph, A.; Bouyssiere, B.; Zhou, H.; Bryant, R. G. Multi-dimensional Nuclear Magnetic Resonance Characterizations of Dynamics and Saturations of Brine/Crude Oil/Mud Filtrate Mixtures Confined in Rocks: The Role of Asphaltene. *Energy Fuels* **2014**, *28* (3), 1629−1640.
(34) Korb, J. P. Multiscale nuclear magnetic relaxation dispersion of complex liquids in bulk and confinement. *Prog. Nucl. Magn. Reson. Spectrosc.* **2018**, *104*, 12−55.
(35) Zavada, T.; Kimmich, R. The anomalous adsorbate dynamics at surfaces in porous media studied by nuclear magnetic resonance methods. The orientational structure factor and Lévy walks. *J. Chem. Phys.* **1998**, *109* (16), 6929−6939.
(36) Stapf, S.; Ren, X.; Talnishnikh, E.; Blumich, B. Spatial distribution of coke residues in porous catalyst pellets analyzed by field-cycling relaxometry and parameter imaging. *Magn. Reson. Imaging* **2005**, *23* (2), 383−6.
(37) Gizatullin, B.; Shikhov, I.; Arns, C.; Mattea, C.; Stapf, S. On the influence of wetting behaviour on relaxation of adsorbed liquids - A combined NMR, EPR and DNP study of aged rocks. *Magn. Reson. Imaging* **2019**, *56*, 63−69.
(38) Silletta, E. V.; Velasco, M. I.; Gomez, C. G.; Strumia, M. C.; Stapf, S.; Mattea, C.; Monti, G. A.; Acosta, R. H. Enhanced Surface Interaction of Water Confined in Hierarchical Porous Polymers Induced by Hydrogen Bonding. *Langmuir* **2016**, *32* (29), 7427−34.
(39) Schauer, G.; Kimmich, R.; Nusser, W. Deuteron field-cycling relaxation spectroscopy and translational water diffusion in protein hydration shells. *Biophys. J.* **1988**, *53* (3), 397−404.
(40) Ayant, Y.; Belorizky, E.; Aluzon, J.; Gallice, J. Calcul des Densités spectrales résultant d'un mouvement aléatoire de translation en relaxation par interaction dipolaire magnétique dans les liquides. *J. Phys. (Paris)* **1975**, *36* (10), 991−1004.
(41) Hwang, L.-P.; Freed, J. H. Dynamic effects of pair correlation functions on spin relaxation by translational diffusion in liquids. *J. Chem. Phys.* **1975**, *63* (9), 4017.
(42) Ayant, Y.; Belorizky, E.; Fries, P.; Rosset, J. Effet des interactions dipolaires magnétiques intermoléculaires sur la relaxation nucléaire de molécules polyatomiques dans les liquides. *J. Phys. (Paris)* **1977**, *38* (3), 325−337.
(43) Freed, J. H. Dynamic effects of pair correlation functions on spin relaxation by translational diffusion in liquids. II. Finite jumps and independent T1 processes. *J. Chem. Phys.* **1978**, *68* (9), 4034−4037.
(44) Merunka, D.; Peric, M. Continuous Diffusion Model for Concentration Dependence of Nitroxide EPR Parameters in Normal and Supercooled Water. *J. Phys. Chem. B* **2017**, *121* (20), 5259−5272.
(45) Peric, I.; Merunka, D.; Bales, B. L.; Peric, M. Rotation of Four Small Nitroxide Probes in Supercooled Bulk Water. *J. Phys. Chem. Lett.* **2013**, *4* (3), 508−513.
(46) Parigi, G.; Ravera, E.; Bennati, M.; Luchinat, C. Understanding Overhauser Dynamic Nuclear Polarisation through NMR relaxometry. *Mol. Phys.* **2019**, *117* (7−8), 888−897.
(47) Wang, X.; Lin, K. S.; Chan, J. C.; Cheng, S. Direct synthesis and catalytic applications of ordered large pore aminopropyl-functionalized SBA-15 mesoporous materials. *J. Phys. Chem. B* **2005**, *109* (5), 1763−9.
(48) Zeidan, R. K.; Hwang, S. J.; Davis, M. E. Multifunctional heterogeneous catalysts: SBA-15-containing primary amines and sulfonic acids. *Angew. Chem., Int. Ed. Engl.* **2006**, *45* (38), 6332−5.
(49) Bennett, A. E.; Rienstra, C. M.; Auger, M.; Lakshmi, K. V.; Griffin, R. G. Heteronuclear decoupling in rotating solids. *J. Chem. Phys.* **1995**, *103* (16), 6951−6958.
(50) Weigler, M.; Winter, E.; Kresse, B.; Brodrecht, M.; Buntkowsky, G.; Vogel, M. Static field gradient NMR studies of water diffusion in mesoporous silica. *Phys. Chem. Chem. Phys.* **2020**, *22* (25), 13989−13998.
(51) Steiner, E.; Bouguet-Bonnet, S.; Blin, J. L.; Canet, D. Water behavior in mesoporous materials as studied by NMR relaxometry. *J. Phys. Chem. A* **2011**, *115* (35), 9941−6.
(52) Wang, X.; Lin, K. S. K.; Chan, J. C. C.; Cheng, S. Direct Synthesis and Catalytic Applications of Ordered Large Pore Aminopropyl-Functionalized SBA-15 Mesoporous Materials. *J. Phys. Chem. B* **2005**, *109* (5), 1763−1769.
(53) Golub, A. A.; Zubenko, A. I.; Zhmud, B. V. γ-APTES Modified Silica Gels: The Structure of the Surface Layer. *J. Colloid Interface Sci.* **1996**, *179* (2), 482−487.
(54) Duvvuri, U.; Goldberg, A. D.; Kranz, J. K.; Hoang, L.; Reddy, R.; Wehrli, F. W.; Wand, A. J.; Englander, S. W.; Leigh, J. S. Water magnetic relaxation dispersion in biological systems: the contribution of proton exchange and implications for the noninvasive detection of cartilage degradation. *Proc. Natl. Acad. Sci. U. S. A.* **2001**, *98* (22), 12479−84.
(55) Sebastiao, P. J.; Sousa, D.; Ribeiro, A. C.; Vilfan, M.; Lahajnar, G.; Seliger, J.; Zumer, S. Field-cycling NMR relaxometry of a liquid crystal above in mesoscopic confinement. *Phys. Rev. E Stat Nonlin Soft Matter Phys.* **2005**, *72* (6 Pt 1), No. 061702.

https://doi.org/10.1021/acs.jpcc.4c00645
J. Phys. Chem. C 2024, 128, 8785−8796